ACS Biomaterials SCIENCE & ENGINEERING

pubs.acs.org/journal/abseba

Article

Surface Engineered PLGA Nanoparticle for Threshold Responsive Glucose Monitoring and "Self-Programmed" Insulin Delivery

Gaurav Ranjan Dey and Arindam Saha*

Cite This: https://doi.org/10.1021/acsbiomaterials.1c00830

Read Online

ACCESS | Metrics & More | Article Recommendations | Supporting Information

ABSTRACT: We have developed a reversible, biocompatible, "self-programmed" PLGA [poly(lactic-*co*-glycolic acid)] nanoparticle-based optical biosensor capable of sensing and continuous monitoring of glucose above the physiologically relevant threshold value (100−125 mg/dL) as well as "on-demand" insulin delivery via an "On−Off" technique. We have carefully surface engineered the PLGA nanoparticle using amino dextran-fluorescein (A-DexFl) and amino-phenyl boronic acid (A-PBA) to exploit the binding affinity of boronic acids with that of *cis*-1,2 diols of dextran/glucose. Initially, the dextran chains wrap the nanoparticle surface due to its high affinity toward A-PBA (K_b = 6.1 × 10^6 M^{-1}). The close proximity of the fluorophores with that of A-PBA quenches the fluorescence, resulting in an "Off" state. On the addition of glucose, it competes with A-DexFl to bind with A-PBA. Above a certain threshold concentration of glucose, the binding affinity overcomes (K_b = 6.3 × 10^7 M^{-1}) the dextran-A-PBA binding. This opens-up the wrapped A-DexFl chains from the nanoparticle surface and results in an increased distance between the fluorophore and A-PBA, triggering the "On" state. The activation of the On−Off state can be finely tuned in the desired range of physiologically relevant glucose concentrations by varying the ligand ratios on the PLGA surface. The nanoparticle core has also been used as an insulin reservoir to trigger the drug release in the "On" state. We have obtained ∼53% encapsulation efficiency and ∼20% loading efficiency for insulin loading. Once the glucose concentration falls beyond the detection range, the dextran chains collapse on the nanoparticle surface with a suspension in drug release. The process is solely controlled by the competition and multivalent binding affinity between glucose, A-DexFl, and A-PBA, which allows it to be "self-programmed" and "self-regulated" with continuous monitoring up to 8−10 cycles over a 72 h time period. A sustained drug release has been found with ∼70% of released drug over a period of 72 h, although this release is insignificant in the absence of glucose. Several control experiments have been performed to optimize the sensor design.

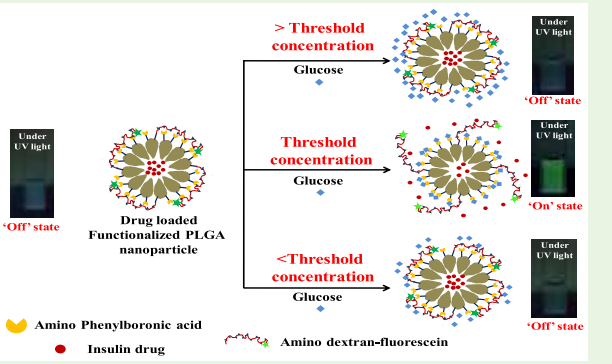

KEYWORDS: *sensor, threshold, self-programmed, functionalized, drug delivery*

INTRODUCTION

Biosensor development have achieved tremendous progress in the last two decades in terms of both selectivity and sensitivity.[1−7] Conventional biosensors like lateral flow immunoassay, enzyme-linked immunosorbent assay (ELISA), fluorescent microarray, polymerase chain reaction (PCR)-based methods, DNA microarray, surface plasmon resonance, etc., require sophisticated technology, expensive equipment, and trained manpower, even though they lack point-of-care detection capability in most cases.[8−12] Thus, simple, portable, inexpensive, miniaturized, and minimally invasive sensors, with point-of-care detection capability, are in high demand. Research in such relevant fields is ongoing at break-neck speeds. In the development of next generation sensors, nanomaterial-based systems have gained remarkable success in recent times.[1−6,9,13−15] The selective and sensitive recognition of the target molecules play a pivotal role in the development of cutting-edge biosensors. Most of the sensors have been developed on the basis of either optical or electrochemical response. Even though electrochemical response is rapid, sensitive, highly accurate, and mitigates background signals, optical response is more favored among scientists due to its ease of detection by the naked eye and simplified fabrication process.[1−3,13,15−22]

Medical tests are often required to detect, diagnose, or monitor various diseases and health issues throughout our life. These include mostly blood tests and different types of imaging. Routine blood tests are often performed as a preventive health check-up or to diagnose and monitor

Received: June 21, 2021
Accepted: August 11, 2021

different disease parameters. These diagnostic tests are aimed at three common outputs: (i) identification of a target species, with either positive or negative responses. These are usually qualitative screening tests to identify the presence of a target species. (ii) The quantification of a target species requires quantitative measurements of the target analyte. The numbers are then compared with the physiologically relevant references of the concerned species to determine abnormalities in the health condition or the onset of diseases. (iii) The continuous monitoring of target analyte evaluates health conditions and monitors a specific target with time.

Among various health issues ravaging our society, diabetes is one of the most relevant and common diseases. It has not only shown a rapidly increasing upward trend but also become a socio global tragedy.[23,24] According to a report, almost half a billion people are living with diabetes, and the number is expected to rise by 51% in 2045.[25] Most people suffer from either type 1 or type 2 diabetes. Diabetes or Diabetes mellitus is a chronic condition that arises due to an elevated level of blood glucose. It is caused either by a declined production of insulin hormone from pancreas gland (type 1 diabetes) or the body cannot use the insulin effectively (type 2 diabetes). Diabetes has been directly linked to cardiovascular disorder, kidney related problems, glaucoma, cancer, HIV, and several other health concerns.[26−28] Other than health concerns, it can indirectly affect the socio-economic burden of a country. Diabetes is not limited to specific countries; rather, it has become a global concern with increasing urbanization and sedentary lifestyle.[29] Diabetes, however, can be controlled and prevented/delayed by a healthy diet, physical exercise, proper medical intervention, and regular check-ups of blood glucose levels. Interestingly, many people are living with diabetes, undetected as the symptoms are not often prominent.[25] Regular monitoring of the blood glucose level is the key to prevent diabetes related complications. Diabetes testing is widely done by collecting blood and testing the sugar level in a laboratory by enzymatic assay.[30,31] This is time-consuming and requires the collection of a blood sample every time, which eventually hinders the rapid and continuous monitoring of blood glucose. To solve this problem, various blood glucose measurement kits are available commercially, which can be easily used by the patients at home. It provides rapid detection, ease of testing, and self-monitoring.[32,33] However, almost all these commercial test strips use glucose oxidase-based electrochemical signaling, which is rapid but requires calibration after every 2−3 tests. Moreover, an enzyme-based system is expensive, lacks reusability, needs optimum storage condition, and requires a blood sample every time to operate. Thus, research focus has been shifted toward the development of continuous glucose monitoring (CGM) devices. Tremendous research has been initiated in the past decade, and many invasive/minimally invasive products are commercially available.[33−36] All these systems are based on an electrochemical signal (amperometric or coulometric) of glucose oxidase-based enzymatic assay. Although these commercial systems can continuously monitor the glucose level, it suffers from high cost, accuracy, low shelf life, calibration issues, etc.[37−39]

Although enzyme-based electrochemical glucose detection is fast, selective, and sensitive, optical methods are being widely explored due to several advantages, like selectivity, easy readout, cost-effective, easy fabrication, avoids repeated calibration, etc. Several optical methods are available for selective and sensitive glucose recognition, including (a) enzymatic detection approach, which undergo changes in their intrinsic optical properties or changes in the labeled fluorophore signal; the recognition of glucose is also possible by the metabolites formed or consumed during reaction of glucose with certain enzymes (e.g., glucose oxidase);[40−43] (b) detection by the interaction with organic or supramolecular boronic acid ligands and associated optical changes;[44−59] (c) specific interaction of glucose with concanavalin A, which undergoes optical changes of labeled fluorophore;[60−62] and (d) interaction with glucose binding proteins and apo-enzymes.[63,64] Among these methods, boronic-acid-based optical detection of glucose and other diols has already attained incredible attention. Various boronic-acid-based molecular architectures have been developed to optimize the sensitivity, selectivity as well as the response time of glucose detection. Multiboronic acid scaffolds, boronic acid modified polymers, self-assembled boronic acid architectures, and boronic acid functionalized nanomaterials have already been widely explored with improved selectivity toward glucose, sensitivity in physiologically important ranges, and fast response time. The major advantages of this system are (a) cost-effective, (b) optical signal readout, (c) easy to control the design and architecture of the scaffold, and (d) reusability of the systems.

Next generation biosensors require the sensing of target biomolecules in the clinically relevant range, typically above the physiologically relevant threshold value (100−125 mg/dL) via an "On−Off" approach by optical means. This minimizes the requirement of digital signal output and frequent calibration and mitigates the cost of enzymatic assay along with the additional advantage of reusability. Thus, the glucose sensor should respond above the physiological threshold value: typically, above 110 mg/dL, i.e., "On" state where the optical signal output can be monitored. Once it is below the threshold value, the sensor will be in the Off state. This response should be specific, fast, and sensitive to the desired glucose level. Moreover, the sensor should be integrated with a "self-programmed" drug reservoir, which can deliver drug only above the threshold glucose level and restrain the release below the threshold level. This On−Off response along with programmed drug release must be continuous within the specific time frame. Various nanomaterials including graphene,[65,66] noble metal nanoparticles,[67,68] silica,[69−71] hydrogels,[65,66,72−76] polymeric nanoparticles,[77−80] and micelles[81−86] have been exploited in the development of glucose responsive drug delivery. However, they lack threshold glucose responsive drug release, continuous monitoring, and reversibility. Among these nanoparticles, we have used PLGA [poly(lactic-*co*-glycolic acid)]-based polymeric nanoparticles due to its biocompatibility, tailored biodegradability, and micellar structure, which can act as a drug reservoir.[87−91]

Here, in this work, we have developed a functionalized PLGA (FPLGA)-based smart and self-programmed biosensor for glucose detection above the physiologically relevant threshold value and simultaneous drug delivery application. We have taken advantage of the competition between dextran and glucose to bind with PBA. We have functionalized the PLGA nanoparticles with amino phenylboronic acid (A-PBA) and amino-dextran fluorescein (A-DexFl) in an optimized ratio via competitive conjugation approach.[92−94] The Off state is achieved via the quenching of fluorescence due to close proximity between boronic acid groups and the fluorophore. The surface modification is tuned in such a way that the On state is achieved only when there is glucose above the

https://doi.org/10.1021/acsbiomaterials.1c00830
ACS Biomater. Sci. Eng. XXXX, XXX, XXX−XXX

Table 1. Monomer Ratio Used to Derive Various Functionalized Nanoparticles (FPLGA) along with Their DLS Size and ζ Potential Values

sample name	molar ratio A-PBA/A-DexFl	concentration of A-PBA (M)	concentration of A-DexFl (M)	DLS size (nm)	ζ potential (mV)
FPLGA-25	25:1	10^{-5}	4×10^{-7}	∼250−300	−40.2
FPLGA-50	50:1	2×10^{-5}	4×10^{-7}	∼250−350	−38.6
FPLGA-75	75:1	3×10^{-5}	4×10^{-7}	∼300−400	−31.6
FPLGA-100	100:1	4×10^{-5}	4×10^{-7}	∼300−450	−25.8
FPLGA-125	125:1	5×10^{-5}	4×10^{-7}	∼350−450	−19.4

Table 2. Ranges of Glucose Concentrations That Were Tested with Various FPLGA Nanoparticles and the Ranges of Glucose Detection Have Been Evaluated

sample name	FPLGA-25	FPLGA-50	FPLGA-75	FPLGA-100	FPLGA-125
glucose concentration tested (mg/dL)	5−100	50−200	80−300	150−400	300−600
glucose concentration detected (mg/dL)	20−80	75−150	110−240	220−350	330−550

physiologically relevant threshold value (typically above 115 mg/dL) and can compete with dextran for binding with PBA. This results in a considerable distance between the fluorophore and boronic acid moiety. As a result, the fluorescence reverts back, achieving the On state. This On−Off state can be achieved repeatedly, allowing for continuous glucose monitoring. A detailed binding constant study has been performed to support this On−Off response. We have also incorporated insulin inside the PLGA nanoparticle core, which acts as a drug reservoir. We have achieved ∼53% encapsulation efficiency and ∼20% loading efficiency. The self-programmed release of the loaded drug can be activated in the On state due to opening up of the caged structure and subsequently deactivated in the Off state due to wrapping up of the caged structure. Several tests have been performed to corroborate the self-programmed drug release with the threshold glucose sensing, thus making it a smart biosensor. We have performed various control tests to achieve the selectivity and sensitivity of the sensor.

EXPERIMENTAL SECTION

Materials and Methods. Poly(D,L-lactide-*co*-glycolide) (PLGA), pluronic F-127, fluorescein-*N*-hydroxysuccinamide (Fluorescein-NHS), fluorescamine, *N*-hydroxysuccinamide (NHS), 1-ethyl-3-(3-(dimethylamino)propyl)carbodiimide (EDC), 4-aminophenylboronic acid hydrochloride (A-PBA), rhodamine B isothiocyanate, insulin from bovine pancreas, D-glucose, D-mannose, D-galactose, fructose, dopamine, sialic acid, glucose oxidase, and cellulose membrane (MWCO ∼ 14 000 Da) were obtained from Sigma and used as received. Amino dextran (MW = 70 000 Da) and dextran (MW = 70 000 Da) were obtained from Invitrogen and used as received. Ethanol, acetone, dichloromethane (DCM), and dimethylformamide (DMF) were obtained from Merck and used as received. Buffer solutions were prepared using buffer capsules (Sigma) following the appropriate method.

Synthesis of Amino Dextran Fluorescein (A-DexFl). Amino dextran (∼5.2 mg, ∼0.075 μM, MW 70 000 Da) was dissolved in 2.5 mL of phosphate buffer (pH 7.4) solution. The solution was then mixed with 300 μL of fluorescein-NHS derivative (∼10 mM prepared in DMF) under mild basic conditions. The final volume was made 3 mL. Fluorescein-NHS derivative was 1.5 times the primary amine concentrations on amino dextran. The mixture was stirred overnight under dark at ∼4 °C. To obtain the A-DexFl, the reaction mixture was mixed with 3.5 mL of ethanol and sonicated until the solution became colorless. The greenish precipitate was collected and washed further with ethanol to remove any unreacted reactants. Finally, the precipitate was dissolved in 3 mL of buffer solution (PBS, pH 7.4) and used as a stock solution.

Test for Primary Amine on A-DexFl. Primary amine test was performed by fluorescamine titration. In brief, a calibration curve was prepared by using standard primary amine solution prepared from glycine in the range 0.1−0.8 mM. Next, 100 μL of A-DexFl stock solution was diluted with water and mixed with 400 μL of freshly prepared fluorescamine solution in acetone. The emission was recorded by exciting at 400 nm. In the case of fluorescein tagged amino-dextran, the emission spectrum was deconvoluted to obtain the contribution from primary amine.

Preparation of PLGA Nanoparticle. PLGA nanoparticle was prepared via an oil-in-water emulsion technique by adapting the literature procedure.[95] PLGA-COOH (∼50 mg) was dissolved in 2 mL of DCM, followed by the dropwise addition (1 mL/min) of the mixture to a solution of pluronic F-127 (200 mg dissolved in 20 mL of water) under sonication. After the complete addition of pluronic F-127, the mixture was further sonnicated for 30 min to yield a milky white solution. The mixture was stirred overnight to remove DCM completely from the solution. The as-prepared nanoparticles were purified by dialysis using a cellulose membrane (MWCO ∼ 14 000 KD). The dialyzed solution was collected and stored for further functionalization.

Functionalization of PLGA Nanoparticle. For functionalization, 2 mL of PLGA nanoparticles was diluted to 3 mL with PBS buffer (pH 7.4). To this solution, 3 mg of EDC was mixed (1 mg/mL) under constant stirring followed by 3 mg of NHS (1 mg/mL). After an hour of reaction, the solution was mixed with 200 μL of A-DexFl (0.007 mM) and 1 mM amino phenyl boronic acid (A-PBA) under constant stirring in the dark. The A-PBA amount was varied according to Table 1. The final volume was kept at 3.5 mL. The reaction was continued overnight and finally dialyzed (cellulose membrane, MWCO ∼ 140 00 KD) against distilled water to remove all the unreacted chemicals. The final volume of the solution was kept at 5 mL.

Test for Glucose with FPLGA Nanoparticle. Nine hundred microliters of the functionalized PLGA (FPLGA) nanoparticle of choice was mixed with 200 μL of glucose solutions (with appropriate dilution), and the final volume was made up to 2 mL. Different glucose concentrations were tested with different FPLGA nanoparticles to maintain a range relevant to the physiologically relevant glucose level (Table 2). After adding glucose, the mixture was incubated for 2−4 h followed by the measurement of fluorescence spectra. Recovered fluorescence was recorded and analyzed.

Continuous On−Off Glucose Detection Test. For this test, 900 μL of FPLGA-75 nanoparticles was mixed with 200 μL of glucose solutions (final concentration: 150 mg/dL), and the final volume was made up to 2 mL. After 2 h of incubation, fluorescence spectra were recorded to obtain the recovered fluorescence. Next, 100 μL of glucose oxidase was added to the solution to oxidize the added glucose. After 30 min of incubation, the nanoparticle solution was centrifuged at 8000 rpm and the precipitate was redispersed in an appropriate amount of buffer solution to keep the dilution factor the same. In this condition, the fluorescence was recorded. This process of alternate addition of glucose and glucose oxidase was repeated 12 times, and on each occasion, fluorescence spectra were recorded.

https://doi.org/10.1021/acsbiomaterials.1c00830
ACS Biomater. Sci. Eng. XXXX, XXX, XXX−XXX

Scheme 1. Preparation of PLGA Nanoparticles, Their Surface Functionalization, and Threshold Responsive Reversible Glucose Sensing via an On−Off-Based Optical Read Out

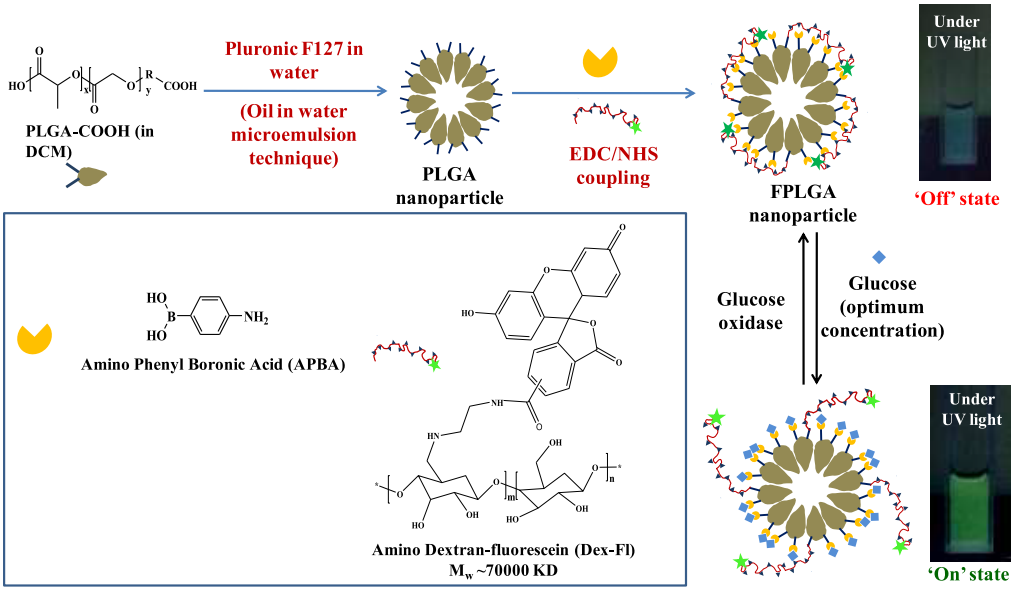

In an alternative approach, no glucose oxidase was used. Only centrifugation was performed at 15 000 rpm, which removes most of the unbound/weakly bound glucose molecules. Then, a similar On−Off study was repeated 12 times.

Control Tests for Glucose Detection. For this test, 900 μL of functionalized PLGA nanoparticles was mixed with 100 μL of different biologically relevant salts and small interfering molecules, resulting in final concentrations of 1 and 10 mM respectively. The sample was stirred for 2 h followed by the measurement of fluorescence spectra. The cations tested are NH_4^+, Na^+, Cu^{2+}, Ca^{2+}, K^+, Fe^{2+}, and Zn^{2+} along with the anions Cl^-, SO_4^{2-}, NO_3^-, and CO_3^{2-}. The small molecules tested are galactose, mannose, fructose, dopamine, and sialic acid. We also studied the control test with a mixture of glucose and fructose, glucose and galactose, and glucose and mannose at various concentrations.

Insulin Loading. For insulin loading, we tagged the insulin with rhodamine B dye to calculate the loading efficiency and monitor the release profile. This tagging was performed by well-known coupling chemistry between the primary amine of insulin and the isothiocyanate of RhB.

To load hydrophilic insulin-RhB to the PLGA nanoparticles, we followed the double emulsion technique. In brief, 25 mg of PLGA was dissolved in 4 mL of DCM followed by the dropwise addition of 200 μL of insulin-RhB under vigorous sonication in ice cold conditions. The sonication was continued until a stable emulsion was formed. The resultant emulsion was added dropwise to a 2 mL pluronic F127 solution (20 mg/mL) under sonication to form the double emulsion. This solution was further added to a 8 mL pluronic F127 solution (20 mg/mL) under vigorous sonication in ice cold conditions. The sonication continued until a stable emulsion was obtained. The final volume was made up to 12 mL by adding water. The solution was kept stirring overnight to completely remove DCM. The final solution was centrifuged at 8000 rpm to remove any free insulin-RhB and surfactants. Finally, the precipitate was dispersed in an equal amount of buffer (pH 7.4). The centrifuge−redispersion was carried out until no emission was found from the supernatant. The drug loaded FPLGA nanoparticles were functionalized using the similar protocol as described above.

Insulin Release Study from FPLGA Nanoparticles. To obtain the drug release profile, insulin loaded FPLGA-75 was treated with glucose solution (150 mg/dL) separately. Each sample was incubated for different time periods starting from 1 to 96 h. After a desired time interval, the drug loaded sample was centrifuged at 8000 rpm and the supernatant was collected. Drug release was observed by fluorescence measurement of the supernatant collected at different time intervals. For a control study, a similar experiment was performed without adding any glucose solution. The drug release profile was also analyzed by varying the glucose concentrations. We used 120, 135, 165, and 180 mg/dL for this study.

On−Off Drug Release Study in Accordance with On−Off Glucose Sensing. For this experiment, we used pure dextran instead of fluorescein tagged dextran to minimize the background emission, keeping all other reaction parameters unchanged. To trigger the drug release, the FPLGA-75 (without tagged fluorescein) was treated with glucose solution (150 mg/dL). After 2 h of incubation, the solution was centrifuged and the supernatant was collected for fluorescence measurement. The precipitate was redissolved and incubated with glucose oxidase for 30 min followed by centrifugation to remove glucose oxidase. The sample thus obtained was further treated with glucose solution. This On−Off process was repeated 10 times before the fluorescence in the supernatant died out.

Control Experiments for Drug Release Study. In a control study, insulin loaded FPLGA-75 was treated with 5 mM galactose, fructose, and mannose separately, and the drug release study was performed at different time intervals. Drug release was studied by photoluminescence measurement of the samples.

In another control study, FPLGA-75 was treated with 100 and 250 mg/dL glucose solution separately. The drug release study was performed via photoluminescence measurement at different time intervals.

Instrumentation. A transmission electron microscopy (TEM) study was performed in a Tecnai G2 30ST (FEI) high resolution transmission electron microscope operating at a voltage of 300 kV. The particle size and ζ potential were measured in a Horiba (SZ-100) analyzer. The photoluminescence properties of the nanoparticles were studied on a steady state spectrofluorometer (QM-40, Photon Technology International, Pvt) using a 150 W xenon lamp. The UV−visible absorbance spectroscopies were performed on an UV−vis-near-IR spectrophotometer (SHIMADZU UV-3600). Fourier transform infrared (FTIR) spectra were performed between 4000 and 400 cm^{-1} on a NICOLET 380 FTIR spectrometer (Thermo Scientific) using a KBr pellet.

https://doi.org/10.1021/acsbiomaterials.1c00830
ACS Biomater. Sci. Eng. XXXX, XXX, XXX−XXX

RESULTS

Synthesis of PLGA Nanoparticles. PLGA nanoparticles were synthesized via an oil-in-water micro emulsion-evaporation technique by adapting the literature method.[96−98] Here, we used acid terminated polylactide-*co*-glycolide polymers (PLGA) having a molecular weight ∼7000−17 000 Da and 50/50 lactide/glycolide ratio as the starting material. Initially the hydrophobic polymer was dispersed in a water immiscible solvent, typically DCM, by vigorous stirring. This solution was mixed with a large volume of water containing stabilizer molecules in a dropwise manner under vigorous sonication. Once the polymer solution interacts with the water, micelle formation initiates with a cloudy appearance. The cloudy solution was further sonnicated for 30 min followed by the evaporation of DCM via overnight stirring (Scheme 1). The final solution was purified via centrifugation followed by dialysis against fresh water with a cellulose membrane (MWCO ∼ 14 000 KD). F-127 (2%) was used as stabilizer to obtain stable nanoparticle with further functionalization ability with the help of surface anchored acid groups of the starting polymer.

Synthesis of Amino Dextran-Fluorescein (A-DexFl). Amino dextran was tagged with fluorescein molecules to study the On−Off performance as well as the binding phenomenon between the carbohydrate molecules and boronic acid groups. Typical amine-NHS conjugation chemistry was adapted to conjugate amino dextran and fluorescein-NHS (Scheme S1) under mild basic conditions in aprotic solvent DMF. The ratio of amino dextran and fluorescein-NHS was kept 2:1 for the conjugation reaction. Free fluorescein molecules, if any, were separated via an ethanol-based precipitation technique, which forcefully precipitates out the dextran molecules from the solution. Optical spectra were obtained to confirm the tagging (Figure S1a). UV−visible spectra clearly indicate the absorption peak at ∼480 nm, whereas the photoluminescence spectra indicate strong emission at ∼530 nm; both are characteristics of fluorescein tagging. We also tested the tagged amino-dextran to confirm the presence of free amine via fluorescamine titration (Figure S1b). Fluorescamine binds to primary amines selectively and generates strong emission in the bluish green region. We obtained a broad spectrum, which after deconvolution demonstrates two separate peaks. The peak at ∼490 nm originates from the fluorescamine test and confirms the presence of free primary amine. The other peak at ∼530 nm originates from the fluorescein tagging. From the fluorescamine titration, we calculated the number of free amines per dextran molecules as well as the percent of tagging (Figures S2 and S3). We found that around 55% of tagging, i.e., around 15 amines per dextran molecule, were tagged with fluorescein. To further confirm the conjugation, we performed the NMR of the conjugated dextran molecules (Figure S4), which provides the characteristic peaks for conjugation.

Functionalization of PLGA Nanoparticles. Acid terminated PLGA nanoparticles were functionalized with amino phenyl boronic acid (A-PBA) and amino dextran fluorescein (A-DexFl) via EDC/NHS coupling chemistry (Scheme 1). Here, we took advantage of the competitive coupling chemistry mentioned elsewhere.[92−94] A-DexFl concentration was kept fixed (0.4 μM), whereas the A-PBA concentration was varied to obtain various functionalized PLGA (FPLGA) nanoparticles (Table 1). Both A-DexFl and A-PBA were prepared separately in the desired concentration followed by the quick addition to the nanoparticle solution. The functionalized PLGA nanoparticle was purified via extensive dialysis. Free A-DexFl was separated by treating with ethanol, which initiates the precipitation of free A-DexFl. Among the various functionalized nanoparticles, we chose FPLGA-50, FPLGA-75, FPLGA-100, and FPLGA-125 for the glucose monitoring study.

Characterization of the Nanoparticles. The nanoparticle size was extensively studied by TEM and DLS study. TEM measurement revealed the nanoparticle size ∼50−125 nm with a wider size distribution (Figure 1a−d) and spherical

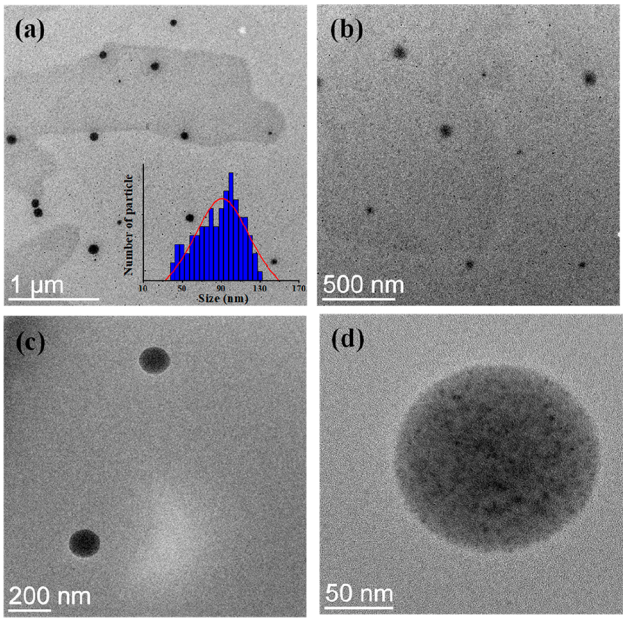

Figure 1. (a−d) TEM images of PLGA nanoparticles in different magnification. The average size varies between ∼50 and 125 nm. The histogram in the inset of (a) shows the average size distribution of the nanoparticles.

shape. The histogram in the inset of Figure 1a shows the overall size distribution of the PLGA nanoparticles as observed in TEM. After functionalization, PLGA nanoparticles retain their shape and size, as observed in TEM (Figure 2a,b). DLS study showed the hydrodynamic diameter of the bare PLGA nanoparticle in the range ∼200−250 nm, whereas functionalized nanoparticles (FPLGA) show a larger size distribution in the range ∼250−450 nm (Figure 3). This wide size distribution is due to the less controlled emulsification method involved in the nanoparticle synthesis. The ζ potential study revealed a high negative surface charge for PLGA nanoparticles (−50 mV), which arises due to terminal acid groups. However, after functionalization, the value gradually decreased to −19.4 mV in FPLGA-125 due to the nonavailability of the acid groups.

The surface characterization of the PLGA and FPLGA nanoparticles was studied by FTIR spectroscopy (Figure 4). Due to the similarities of surface functional groups, both the FTIR spectra provide almost similar characteristics. The strong peak at 3452 cm^{-1} arises from the —OH stretching frequency of the PLGA nanoparticles, which further enhances after functionalization due to dextran molecules. The major peak at 2930 cm^{-1} arises due —C—H symmetric stretching, which is found in both spectra. The small peak at 2992 cm^{-1} is due to

https://doi.org/10.1021/acsbiomaterials.1c00830
ACS Biomater. Sci. Eng. XXXX, XXX, XXX−XXX

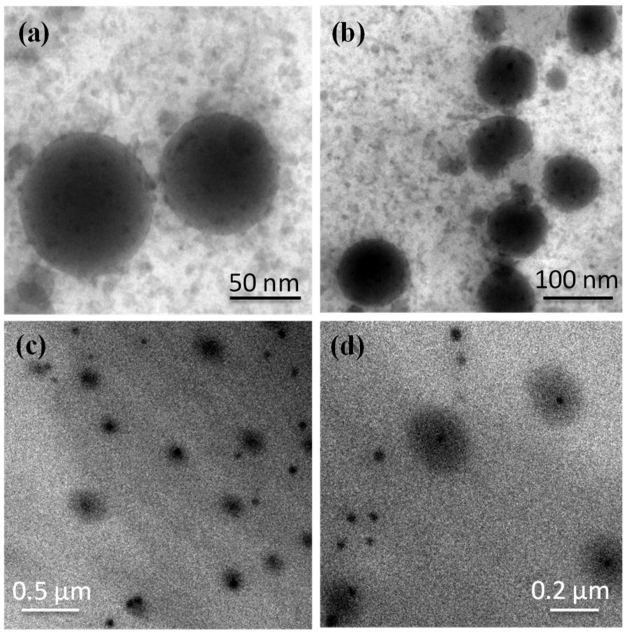

Figure 2. (a and b) TEM images of functionalized PLGA nanoparticles (FPLGA) in two different magnifications. The average size varies between ∼50 and 125 nm, which indicates no appreciable size change after functionalization. (c and d) TEM size distribution of insulin loaded FPLGA nanoparticles. The size ranges from ∼150 to 300 nm with some smaller PLGA nanoparticles. The larger size is due to the double emulsion synthesis technique.

—C—H asymmetric stretching, which is observed in PLGA nanoparticles. The strong peak at 1770 cm^{-1} arises because of the —C═O stretching vibration of the PLGA nanoparticles, which is sharper in functionalized nanoparticles due to the amide I contribution from the amino dextran molecules. The peak at 1620 cm^{-1} contributes toward —COO stretching frequency in both cases. The weak peak at 1384 cm^{-1} arises due to —C—H deformation in PLGA nanoparticles, which is strong and sharp in the case of functionalized nanoparticles due to boronate ester formation. The peaks at 1200 and 1132 cm^{-1} arise due to —CH_3 skeletal vibration and —C—O stretching vibration, respectively, in both cases. The peaks below 1000 cm^{-1} arise mostly due to C—O rocking vibration and CH_3CO skeletal vibration of the surfactants, which is less prominent in FPLGA nanoparticles due to functionalization. However, a sharp peak was observed at 657 cm^{-1} for FPLGA nanoparticles, which is attributed to the —B—O stretching of the boronate esters.[99] This peak is absent in the case of PLGA nanoparticles.

Fluorescence spectra analysis of the functionalized PLGA nanoparticles reveals the quenching of fluorescence in all the samples (Figure 5). The quenching is in the order of 100 in almost all the cases except FPLGA-25, where the quenching is the least. Control fluorescence obtained from A-DexFl functionalized PLGA nanoparticles, without adding any A-PBA. The digital images of the samples do not show any indicative emission as observed by naked eye (Figure 5a) compared to the control sample.

Glucose Detection Tests. We optimized FPLGA-25, FPLGA-50, FPLGA-75, FPLGA-100, and FPLGA-125 after several experiments. We tested the samples with different amounts of biologically relevant glucose concentrations, and after the optimization process, we attained a range of glucose concentration that were detected by these FPLGA nanoparticles (Figure 6 and Table 2) via fluorescence On−Off technique. We observed that FPLGA-25 successfully recovers the quenched fluorescence when treated with glucose solutions in the concentration range 20−80 mg/dL, much lower than the physiologically relevant threshold value. FPLGA-50 and FPLGA-75 responses to the glucose concentration range between 75 and 150 and 115 and 240 mg/dL, respectively. Similarly, FPLGA-100 and FPLGA-125 effectively recover the quenched fluorescence in the ranges 220−350 and 330−550 mg/dL glucose concentration, respectively. However, this fluorescence recovery does not follow any linear trend. Initially, it increases gradually and attains peaks at a certain glucose concentration followed by a gradual decrease in PL intensity. The digital images of all the samples for recovered fluorescence were studied. It has been observed that no visible fluorescence was detected beyond the specific ranges of FPLGA, as mentioned in Table 2.

For control study, we tested galactose, mannose, fructose, sialic acid, and dopamine among the small biologically interfering molecules (Figure S5a). We observed no significant recovered fluorescence in all the cases compared to glucose. Among the salts, we tested NH_4^+, Na^+, Cu^{2+}, Ca^{2+}, K^+, Fe^{2+}, and Zn^{2+} as the cations and Cl^-, SO_4^{2-}, NO_3^-, and CO_3^{2-} as the anions since they are physiologically relevant. Here also, we did not observed any significant fluorescence recovery (Figure S5b) compared to glucose. In each case, we incubated the FPLGA-75 nanoparticles with the sample for 4 h and centrifuged, followed by fluorescence measurement. To understand the interference of other *cis*-diols of interest, we further studied the glucose detection with a mixture of cis-diols. Here, we studied the recovered fluorescence of a mixture of glucose−fructose, glucose−galactose, and glucose−mannose at various concentrations (Figure S5c).

Binding Constant Study. To evaluate the binding constant between boronic acid and glucose molecules as well as dextran molecules, we treated the functionalized PLGA (FPLGA-75) nanoparticles with varying concentrations of glucose (typically between 115 and 125 mg/dL) separately followed by 3 h of incubation. After centrifugation, the supernatant was studied for the recovered fluorescence (Figure S6). Similarly, to find the binding constant between dextran and PBA molecules, we functionalized the PLGA nanoparticles by varying the A-DexFl concentration and studied the quenching of Dex-Fl via fluorescence measurement. In both the cases, we adapted a 1:1 ligand binding model to calculate the binding constant values (Figure S7). It is observed that the binding constant between glucose and PBA molecules (6.3×10^7 M^{-1}) is almost 10 times higher than the binding constant between PBA and dextran molecules (6.1×10^6 M^{-1}) under the measured range of study. Each sample was tested five times, and the relative standard deviation was measured between 1 and 3%.

Continuous Glucose Monitoring Study. For continuous glucose monitoring, we used two different methods. In the first method, we used glucose oxidase to oxidize glucose molecules, once the positive response was detected. The treated sample was centrifuged thoroughly followed by fluorescence measurement, which reflects the Off state. Again, the sample was treated with an appropriate amount of glucose to trigger the On state further. This On−Off phenomenon was repeated for 12 times in a 72 h period to confirm its effectiveness for a longer duration (Figure 7). In the figure, the Off state is shown

https://doi.org/10.1021/acsbiomaterials.1c00830
ACS Biomater. Sci. Eng. XXXX, XXX, XXX−XXX

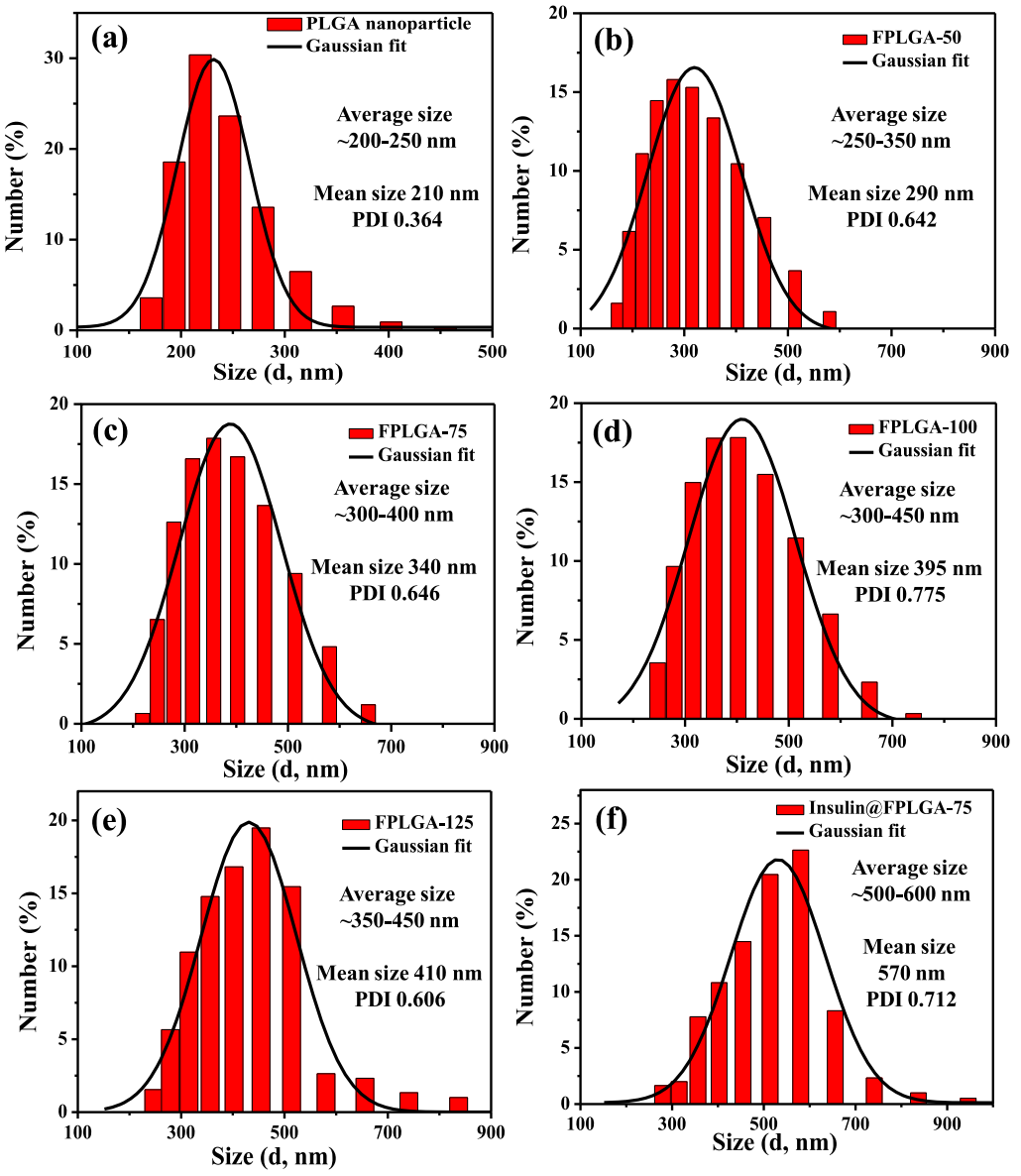

Figure 3. Hydrodynamic size of the (a) PLGA and (b−e) FPLGA nanoparticles were studied via DLS measurement. PLGA nanoparticles exhibited ∼200−250 nm sizes, whereas FPLGA nanoparticles exhibited sizes in the range ∼250−450 nm depending on the surface functionalization. (f) Insulin loaded FPLGA75 nanoparticles exhibited sizes in the range ∼500−600 nm. The mean size of each DLS plot along with its PDI value is mentioned in each graph.

to have no green emission whereas the On state has visible green emission under UV irradiation. However, the On state is not uniform as clearly observed from the graph. The digital image in every step further confirms this On−Off response. In another method, we only centrifuged the solution at 15 000 rpm once the On state was reached without adding any enzyme. The precipitate was collected and fluorescence was measured, which represents the Off state. Although here the Off state is less prominent compared to the previous method (Figure S8), the On−Off response can still be detected under UV irradiation.

Drug Loading and Release Study. To study the drug loading and the "On-demand" drug release study, we incorporated insulin in the core of FPLGA nanoparticles via a double emulsion technique (Figure 2c,d and Figure S9). To track the colorless drug for loading and releasing purpose, we tagged it with rhodamine B via amine-isothiocyanate coupling (Ins-RhB) and used it instead of pure insulin (Scheme S2). The tagging was confirmed via optical study (Figure S10). Drug loading was studied via UV−visible spectroscopy and it was found at almost 53% encapsulation efficiency, whereas the loading capacity was obtained at ∼20% (Figure 8a, Figure S11). In the UV−visible spectra, the absorbance observed at ∼550 nm in the drug loaded sample is due to the tagged insulin loaded inside the nanoparticle.

To perform the drug release study, insulin loaded PLGA nanoparticle was functionalized according to FPLGA-75, where we used untagged amino dextran molecules instead of fluorescein tagged ones (Scheme S2). Drug release was performed in the presence of glucose and in the absence of glucose. In presence of glucose, samples were collected at different time intervals of 3, 6, 12, 24, 36, 48, and 72 h, respectively. The percent release was plotted against time and found to have a sustained release up to 48 h, which gets

https://doi.org/10.1021/acsbiomaterials.1c00830
ACS Biomater. Sci. Eng. XXXX, XXX, XXX−XXX

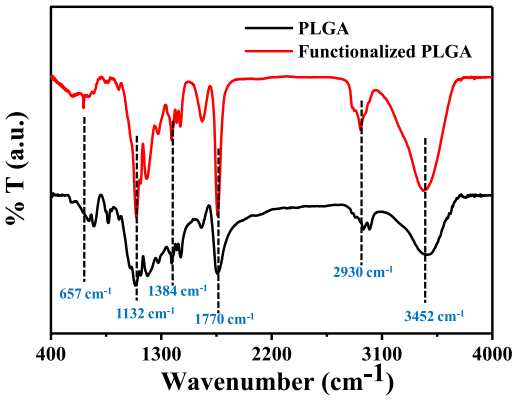

Figure 4. FTIR spectra of PLGA nanoparticles (black) and FPLGA nanoparticles (red) with characteristic peaks. The strong peak at 3452 cm^{-1} arises from the —OH stretching frequency of PLGA nanoparticles, which further enhances after functionalization due to dextran molecules. The major peak at 2930 cm^{-1} arises due to —C—H symmetric stretching, which is found in both spectra. The strong peak at 1770 cm^{-1} arises because of the —C═O stretching vibration of the PLGA nanoparticles, which is sharper in functionalized nanoparticles due to the amide I contribution from the amino dextran molecules. The peak at 1620 cm^{-1} contributes toward —COO stretching frequency in both cases. The weak peak at 1384 cm^{-1} arises due to —C—H deformation in PLGA nanoparticles, which is strong and sharp in the case of functionalized nanoparticles due to boronate ester formation. The peaks at 1200 and 1132 cm^{-1} arise due to —CH_3 skeletal vibration and —C—O stretching vibration, respectively, in both cases. The peak at ∼657 cm^{-1} in FPLGA is the distinctive characteristics of boronate ester, which is absent in PLGA nanoparticles.

saturated over a 72 h time period (Figure 8b). Whereas a similar study was performed without adding glucose, so no significant drug release was obtained. As a control, we also studied the drug release by adding fructose, mannose, and galactose separately at similar concentrations as glucose (Figure S12a); however, no detectable drug release was found. In another control experiment, drug release was performed under lower and higher glucose concentration than the optimum range of detection to optimize the drug release performance. In this case, we studied the release of FPLGA-75 with 100 mg/dL glucose and 250 mg/dL glucose, which demonstrates insignificant drug release (Figure S12b).

"On-Demand" Drug Release Study. The release study was performed using insulin loaded FPLGA-75 where the functionalization uses amino-dextran instead of A-DexFl. This study was performed exactly the same way it was performed for the On−Off glucose responsive study. The sample was treated with 150 mg/dL glucose and incubated for 3 h followed by centrifugation. The supernatant was collected, and fluorescence spectra were measured to obtain the amount of released drug. This corresponds to the On state. The precipitate was treated with glucose oxidase followed by centrifugation. The supernatant was collected, and fluorescence was recorded. This corresponds to the Off state. We repeated the cycle five times over a period of 48 h, following which, drug release was insignificant (Figure 9). The digital images (Figure 9) exhibit this On−Off drug release in the presence of an optimum amount of glucose.

DISCUSSION

We intended to develop a "self-operating" smart nanosensor for glucose, which can switch on above the physiologically relevant threshold blood glucose level (110−125 mg/dL) and switch off automatically once the level is out of the sensing range. Moreover, we intended to associate this On−Off response with the release of insulin in a self-programmed manner. Whenever the blood glucose level is elevated, the sensor system will trigger the drug release automatically and suspend release once the level falls below the threshold level. For this purpose, we adapted the very well-known concept of multivalent-interaction and competitive binding.[86,87] It is well-studied that boronic acids and aryl boronic acids along with their counterparts have a high affinity toward *cis*-1,2- and 1,3-diols, which have specific advantages for monosaccharide detection and monitoring.[58,59] This concept has been widely used, and many studies have been performed. However, it lacks (i) self-monitoring capability, (ii) threshold responsiveness via On−Off output, (iii) self-programmed insulin release, and (iv) reversible but sustained insulin delivery (Table S1). Another challenge is to make this sensing feasible under physiological pH (7.4), as the pK_a of boronic acid-diol reaction falls above 8.0.

In our study, we used conventional PLGA nanoparticles since they are biocompatible and biodegradable nanoparticles, approved by the FDA.[81−85] The PLGA nanoparticles, synthesized via a microemulsion technique, are spherical in shape and have a size distribution in the range ∼50−125 nm. These PLGA nanoparticles, synthesized using acid terminated monomers, render free acid groups on its surface, which have been further exploited for competitive conjugation. We have developed and extensively studied competitive conjugation, which can control the ligand density of a target ligand of choice on a nanoparticle surface.[92−94] Here, we used two different

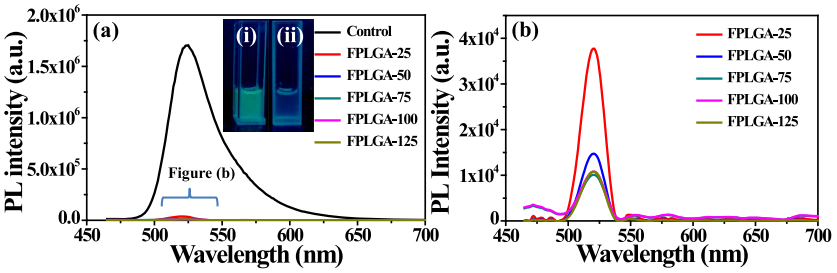

Figure 5. (a) Photoluminescence spectra of the functionalized PLGA nanoparticles having various ratios of A-DexFl and A-PBA. Here, control spectra represent FPLGA without adding A-PBA. The bracketed portion in (a) is enlarged in graph (b). The spectra clearly represent the fluorescence quenching of the functionalized samples. The inset images of (a) represent the digital photograph of the control sample (i) and FPLGA-75 (ii) under UV light.

https://doi.org/10.1021/acsbiomaterials.1c00830
ACS Biomater. Sci. Eng. XXXX, XXX, XXX−XXX

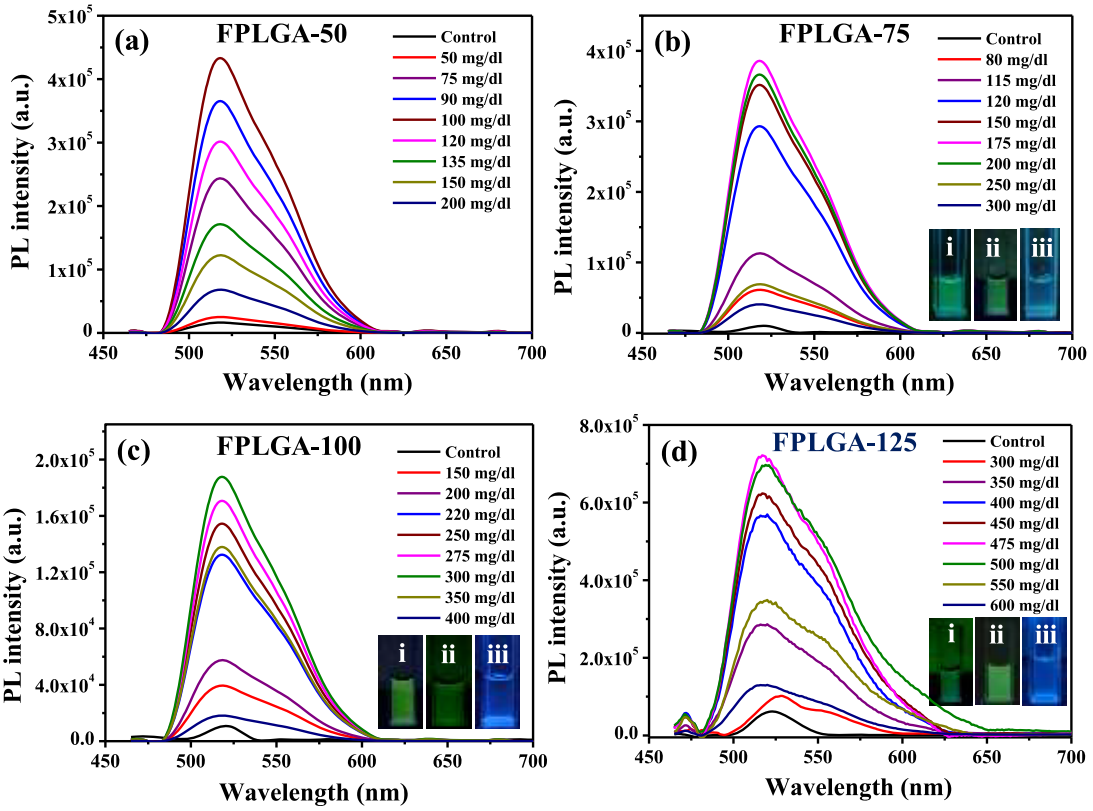

Figure 6. Recovered PL spectra of the various functionalized PLGA nanoparticles upon glucose treatment. (a) Recovered PL of FPLGA-50 upon treatment with 50−200 mg/dL glucose solution, (b) FPLGA-75 upon treatment with 80−300 mg/dL glucose solution, (c) FPLGA-100 upon treatment with 150−400 mg/dL glucose solution, and (d) FPLGA-125 upon treatment with 300−600 mg/dL glucose solution. The digital images in the insets of (b−d) demonstrate the recovered fluorescence under UV light, visible via the naked eye. The inset digital image of (b) indicates recovered fluorescence upon treatment with 120 (i), 200 (ii), and 300 mg/dL (iii) glucose, respectively. Similarly, the digital images in the inset of (c) represent the recovered fluorescence upon treatment with 250 (i), 350 (ii), and 400 mg/dL (iii) glucose, respectively. In (d), the inset digital images represent recovered fluorescence upon treatment with 400 (i), 500 (ii), and 600 mg/dL (iii) glucose, respectively.

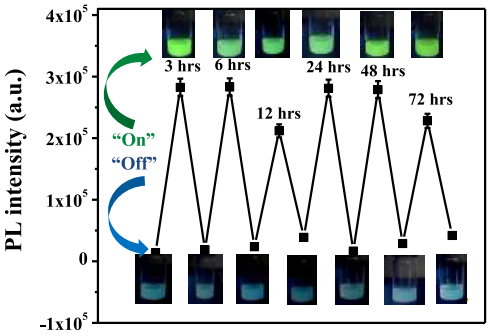

Figure 7. Threshold glucose responsive fluorescence On−Off study. The study has been conducted using FPLGA-75 in the presence of 150 mg/dL glucose. In presence of glucose, recovered fluorescence corresponds to the On state. The Off state is triggered using glucose oxidase. This On−Off cycle was repeated six times during a 72 h period. In each step, a digital image was recorded to support the observed data. The relative standard deviation was found to be ∼3−5%.

ligands, amino phenyl boronic acid (A-PBA) and amino dextran-fluorescein (A-DexFl). EDC/NHS coupling chemistry was adopted for the conjugation of the ligands. This controlled functionalization allowed for placing A-PBA and A-DexFl in such a way that the *cis*-diol groups of the dextran get attached with the diols of the A-PBA in a selective manner. As a consequence, the FPLGA nanoparticle gets wrapped with dextran molecules and the attached fluorophore comes in close proximity with the A-PBA leading to the quenching of fluorescence (Figure 5). This dextran−PBA interaction has several advantages toward the threshold glucose sensing: (1) the boronate ester formed between dextran and PBA and brings down the pK_a value for the glucose−PBA interaction, and thus, the sensing can be operated under a physiological pH. (2) This multivalent interaction has a higher binding affinity compared to single glucose−PBA binding, which helps in keeping the binding intact until and unless there is sufficient glucose concentration to overcome the binding affinity. (3) This interaction also quenches the fluorescence of the tagged fluorophore, facilitating the On−Off response.

When glucose solution is added to the FPLGA solution, the glucose molecules start a competition with the dextran molecules to bind with the PBA moieties. But, due to a higher binding affinity (multivalency) between dextran and PBA, glucose binding is unsuccessful. The binding affinity between dextran and PBA was calculated to be 6.1×10^6 M^{-1}. If we keep on increasing the glucose concentration, after a certain concentration (threshold concentration), there is sufficient glucose molecules and the binding affinity between glucose and PBA (6.3×10^7 M^{-1}) just overcomes the affinity between dextran and PBA. Thus, the dextran molecule gets released, and due to this increased distance between tagged fluorophore and PBA molecules, the fluorescence reverts back, which indicates the On state (Figure 6). The release of dextran

https://doi.org/10.1021/acsbiomaterials.1c00830
ACS Biomater. Sci. Eng. XXXX, XXX, XXX−XXX

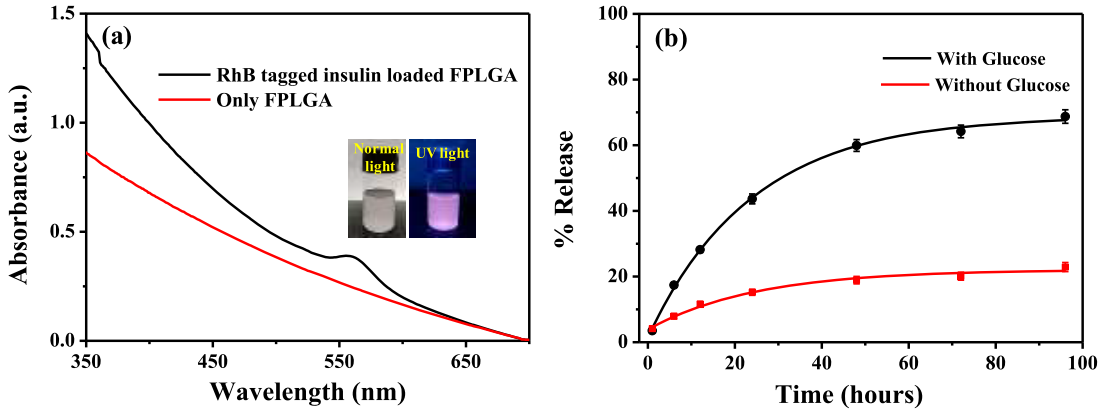

Figure 8. (a) Drug loading was identified by comparing the UV−visible spectra of the FPLGA nanoparticles and drug loaded nanoparticles. Insulin was tagged with rhodamine B, which shows prominent absorption at 560 nm. (b) Drug release profile was obtained by treating the drug loaded FPLGA-75 with 150 mg/dL glucose solution and incubated for a desired time interval separately. The released drug was plotted against time, which exhibits saturation in a released drug at about 72 h. For the control, drug release was also performed without adding any glucose, which exhibits ∼20% drug release.

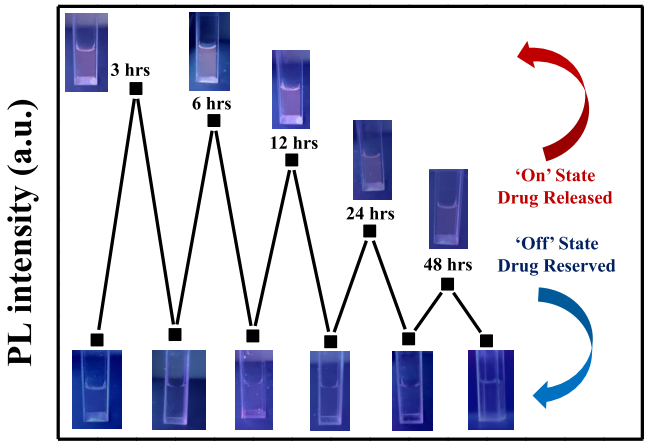

Figure 9. Threshold glucose responsive self-programmed drug release study using RhB tagged insulin as a drug. FPLGA-75 was taken as the nanoparticle under study, which was treated with 150 mg/dL glucose. Released drug was separated and quantified as On state. The sample was treated with glucose oxidase to induce the Off state. The same sample was further treated with a desired amount of glucose, and the released drug was quantified. The cycle continued for five times over a 48 h period. All the digital images were collected from the supernatant after centrifuging out the drug loaded FPLGA nanoparticles.

molecules from the nanoparticle surface can be detected via DLS measurement. An increase in hydrodynamic diameter (∼900−1000 nm) was found due to opening up the wrapped structure (Figure S13). In both the bindings, multivalent interaction plays the pivotal role.

Although, the dextran gets detached from the PBA, it is still attached with the nanoparticle via covalent linkage, which in turn provides the reversibility in the system. Once the glucose concentration falls below the threshold limit, the binding affinity between dextran and PBA become stronger again and thus brings back the Off state. If we carefully observe the recovered fluorescence (Figure 6), it has been found that, after the threshold limit, the recovered fluorescence starts to increase with increasing glucose concentration, although this increase is not linear over the entire range (Figure S14). This can be explained by the competitive binding phenomenon between A-DexFl and glucose for PBA. Since after threshold concentration, glucose−PBA binding constant overcomes the dextran−PBA binding, most of the dextran detaches from the PBA simultaneously and thus a linear response is not obtained for the entire range. However, the fluorescence is increased with increasing glucose concentration as more and more dextran gets detached due to a lowering of binding affinity until a maximum is reached. Surprisingly, after the maxima, fluorescence starts quenching again and completely quenches above a certain upper limit (Figure S14). To explain this, we must keep in mind that glucose and PBA binding follows a 1:2 binding event. The 1,2- and 5,6-*cis*-diols of glucose in their glucofuranose form binds with two adjacent PBA molecules. Once the glucose concentration increases to a large extent, glucose density into the vicinity of the PBA molecules increases. Due to the dynamic nature of the binding, excess glucose forces each glucose to bind with a single PBA molecule, thus following a 1:1 binding model. This, 1:1 binding has a much lower binding affinity, and thus, dextran−PBA binding can overcome glucose−PBA binding and return back to the Off state.

These upper limits of detection provide great advantage for the development of a qualitative sensor with quantitative output. We have finely tuned the surface of PLGA nanoparticles by varying the ratio of A-PBA and A-DexFl (Table 1). A higher multivalent interaction between PBA moiety and dextran shifts both the lower and upper detection limits to the higher side (Table 2). We have developed four different such sensor nanostructures by controlled surface modification, which operate in an On−Off manner in different detection ranges. This alleviates the need of quantitative measurement by a digital signal as the qualitative range of detection provides quantitative output.

We studied this On−Off glucose detection over a period of 72 h with specific time intervals (Figure 7). To create the Off state in vitro, we used glucose oxidase, which oxidizes glucose to glucono-1,5-lactone and thus has no binding preference toward PBA. Glucose oxidase also exhibits green emission. To remove the excess enzyme as well as the generated hydrogen peroxide, the sample was centrifuged. The FPLGA precipitates out, which was thoroughly washed before proceeding to the next cycle. After 6−8 cycles, the FPLGA nanoparticles lose their stability due to repeated washing and redispersion.

To observe the reversible and glucose responsive On−Off drug release, we incorporated insulin drug into the FPLGA

https://doi.org/10.1021/acsbiomaterials.1c00830
ACS Biomater. Sci. Eng. XXXX, XXX, XXX−XXX

nanoparticle via a double emulsion technique. Since, insulin is colorless, we tagged insulin with rhodamine B isothiocyanate via covalent conjugation. The tagging was confirmed and quantified via optical spectra (Figures S10 and S11). This will help to quantify and observe the loading and release profile of the drug. Calculation reveals the ∼3.5 rhodamine B was tagged to each insulin molecule. To functionalize this drug loaded PLGA nanoparticle, we used the same ratio of A-PBA and A-Dex as optimized (Table 1). However, here we used only amino dextran of same molecular weight rather than the fluorescein tagged one to avoid any confusion of emission overlapping. Drug loading was estimated as ∼53% encapsulation efficiency and ∼20% loading efficiency (Figure S11). Loading efficiency was optimized after performing several experiments. The addition of a higher amount of drug initiates instability in the emulsion formation and thus lowers the encapsulation efficiency. A lower loading efficiency is due to a higher molecular weight of the PLGA nanoparticles, which minimizes the amount of drug per milligram of sample. Drug release was performed in the presence and absence of optimum glucose solution. In presence of glucose, the nanoparticles achieved sustained drug release and saturated over 72 h with ∼70% drug release. This is important, as the rapid release of drug above the threshold glucose level may cause physiological issues. This saturation is obtained when the dextran wrapping remains open for 72 h continuously. In the On−Off experiment, drug release is much less in every consecutive On state and depends on the period the gate has been open. The longer the gate remains open, the more drug would release and interact with the elevated glucose level. This is particularly important in the self-programmed bio sensor, which avoids the manual intervention. It has also been observed that drug release is insignificant above (∼20%) and below (∼15%) the optimum range of operation (Figure S12b). In the absence of glucose, this release has been found to be as low as ∼20%. We also tested the release with other carbohydrates, where drug release was found irrelevant (Figure S12a). We also studied the glucose responsive On−Off reversible drug release, where the released drug in the On state was found to decrease gradually with time (Figure 9). This can be explained by the limited capacity of the reservoir, which was exploited in the cycle. With each cycle, loaded reserved drug gets expended, which eventually affects the amount of dug released in the next cycle. However, this drug release is in accordance with the glucose responsive On−Off study and thus can be utilized in a self-regulating glucose responsive drug delivery approach.

CONCLUSION

In conclusion, we have developed functionalized PLGA-based smart nanoparticles to regulate and monitor the glucose level above the physiological relevant level via an On−Off approach. This approach is self-regulating, and once the glucose level crosses the threshold value, it generates a fluorescence signal. This triggers the release of drug, insulin, in a sustained manner. Once the glucose level falls below the threshold value, the signal goes back to the Off state and drug release is suspended. This has been achieved via the competitive conjugation of A-PBA and A-DexFl on the nanoparticle surface. The phenyl boronic acid molecules bind with dextran molecules due to high multivalent interaction with the quenching of fluorescence. However, in the presence of sufficient glucose, PBA tends to bind with glucose molecules once the binding affinity with dextran is compromised. This opens up the nanoparticle surface, leading to the recovery of fluorescence and subsequent drug release. The process is reversible and can act as a continuous glucose monitoring system. We believe that this self-regulating approach can solve the shortcomings of existing "continuous glucose monitoring" devices along with self-regulated insulin shots without the need of digital signal output. This biosensor is simple, cost-effective, sensitive, selective, and tunable. Finally, this approach can be further exploited to monitor other biological and pathological phenomenons and have immense sensing and therapeutic capabilities without any manual intervention.

ASSOCIATED CONTENT

Supporting Information

The Supporting Information is available free of charge at https://pubs.acs.org/doi/10.1021/acsbiomaterials.1c00830.

Schemes of synthetic pathway and On−Off reversible technique, table of phenyl-boronic-acid-based nanosystems, and figures of UV−visible and photoluminescence spectra, calibration curve for amine determination, presence of primary amine, calculation to obtain the percent of fluorescein tagging of A-DexFl, NMR spectra, control tests, recovered fluorescence, dissociation constants, fluorescence quenching, binding constant calculation, On−Off glucose response, TEM images, calculation of tagged RhB per insulin molecule and drug loading calculation, drug release study, DLS study, and glucose concentration is plotted against recovered fluorescence (PDF)

AUTHOR INFORMATION

Corresponding Author

Arindam Saha − *Functional Materials and Devices Division, CSIR-Central Glass and Ceramic Research Institute, Kolkata 700032, India;* orcid.org/0000-0002-0207-7971; Phone: 91-33-2483 7340 (Extension 3217); Email: arindamchemiitkgp@gmail.com

Author

Gaurav Ranjan Dey − *Functional Materials and Devices Division, CSIR-Central Glass and Ceramic Research Institute, Kolkata 700032, India;* Present Address: Department of Chemistry, The Pennsylvania State University, University Park, Pennsylvania 16802, United States

Complete contact information is available at: https://pubs.acs.org/10.1021/acsbiomaterials.1c00830

Notes

The authors declare no competing financial interest.

ACKNOWLEDGMENTS

A.S. acknowledges the Department of Science and Technology (DST), India for providing a research grant (DST INSPIRE Faculty Research Grant, Project No. GAP 0364).

REFERENCES

(1) Anker, J. N.; Hall, W. P.; Lyandres, O.; Shah, N. C.; Zhao, J.; Van Duyne, R. P. Biosensing with Plasmonic Nanosensors. *Nat. Mater.* **2008**, *7*, 442−453.

(2) Shao, Y.; Wang, J.; Wu, H.; Liu, J.; Aksay, I. A.; Lin, Y. Graphene Based Electrochemical Sensors and Biosensors: A Review. *Electroanalysis* **2010**, *22*, 1027−1036.
(3) Saha, K.; Agasti, S. S.; Kim, C.; Li, X.; Rotello, V. M. Gold Nanoparticles in Chemical and Biological Sensing. *Chem. Rev.* **2012**, *112*, 2739−2779.
(4) Ispas, C. R.; Crivat, G.; Andreescu, S. Review: Recent Developments in Enzyme-Based Biosensors for Biomedical Analysis. *Anal. Lett.* **2012**, *45*, 168−186.
(5) Saha, A.; Jana, N. R. Detection of Cellular Glutathione and Oxidized Glutathione Using Magnetic−Plasmonic Nanocomposite-Based "Turn-Off" Surface Enhanced Raman Scattering. *Anal. Chem.* **2013**, *85*, 9221−9228.
(6) Saha, A.; Jana, N. R. Paper Based Microfluidic Approach for Surface-Enhanced Raman Spectroscopy and Highly Reproducible Detection of Proteins beyond Picomolar Concentration. *ACS Appl. Mater. Interfaces* **2015**, *7*, 996−1003.
(7) Vigneshvar, S.; Sudhakumari, C. C.; Senthilkumaran, B.; Prakash, H. Recent Advances in Biosensor Technology for Potential Applications − An Overview. *Front. Bioeng. Biotechnol.* **2016**, *4*, 1−9.
(8) Kroh, E. M.; Parkin, R. K.; Mitchell, P. S.; Tewari, M. Analysis of Circulating MicroRNA Biomarkers in Plasma and Serum Using Quantitative Reverse Transcription-PCR (qRT-PCR). *Methods* **2010**, *50*, 298−301.
(9) Peng, G.; Hakim, M.; Broza, Y. Y.; Billan, S.; Abdah-Bortnyak, R.; Kuten, A.; Tisch, U.; Haick, H. Detection of Lung, Breast, Colorectal, and Prostate Cancers from Exhaled Breath Using a Single Array of Nanosensors. *Br. J. Cancer* **2010**, *103*, 542−551.
(10) Schrader, C.; Schielke, A.; Ellerbroek, L.; Johne, R. PCR Inhibitors − Occurrence, Properties and Removal. *J. Appl. Microbiol.* **2012**, *113*, 1014−1026.
(11) Gan, S. D.; Patel, K. R. Enzyme Immunoassay and Enzyme-Linked Immunosorbent Assay. *J. Invest. Dermatol.* **2013**, *133*, 1−3.
(12) Kuhle, J.; Barro, C.; Andreasson, U.; Derfuss, T.; Lindberg, R.; Sandelius, A.; Liman, V.; Norgren, N.; Blennow, K.; Zetterberg, H. Comparison of Three Analytical Platforms for Quantification of the Neurofilament Light Chain in Blood Samples: ELISA, Electrochemiluminescence Immunoassay and Simoa. *Clin. Chem. Lab. Med.* **2016**, *54*, 1655−1661.
(13) Zhang, C. Y.; Yeh, H. C.; Kuroki, M. T.; Wang, T. H. Single-Quantum-Dot-Based DNA Nanosensor. *Nat. Mater.* **2005**, *4*, 826−831.
(14) Wang, S.; Lin, L.; Wang, Z. L. Triboelectric Nanogenerators as Self-Powered Active Sensors. *Nano Energy* **2015**, *11*, 436−462.
(15) Mitra, R.; Saha, A. Reduced Graphene Oxide Based "Turn-On" Fluorescence Sensor for Highly Reproducible and Sensitive Detection of Small Organic Pollutants. *ACS Sustainable Chem. Eng.* **2017**, *5*, 604−615.
(16) Grieshaber, D.; MacKenzie, R.; Voros, J.; Reimhult, E. Electrochemical Biosensors - Sensor Principles and Architectures. *Sensors* **2008**, *8*, 1400−1458.
(17) Dolatabadi, J. E. N.; Mashinchian, O.; Ayoubi, B.; Jamali, A. A.; Mobed, A.; Losic, D.; Omidi, Y.; de la Guardia, M. Optical and Electrochemical DNA Nanobiosensors. *TrAC, Trends Anal. Chem.* **2011**, *30*, 459−472.
(18) Kimmel, D. W.; LeBlanc, G.; Meschievitz, M. E.; Cliffel, D. E. Electrochemical Sensors and Biosensors. *Anal. Chem.* **2012**, *84*, 685−707.
(19) Mondal, A.; Sinha, A.; Saha, A.; Jana, N. R. Tunable Catalytic Performance and Selectivity of a Nanoparticle−Graphene Composite through Finely Controlled Nanoparticle Loading. *Chem. - Asian J.* **2012**, *7*, 2931−2936.
(20) Zhai, D.; Liu, B.; Shi, Y.; Pan, L.; Wang, Y.; Li, W.; Zhang, R.; Yu, G. Highly Sensitive Glucose Sensor Based on Pt Nanoparticle/Polyaniline Hydrogel Heterostructures. *ACS Nano* **2013**, *7*, 3540−3546.
(21) Pashchenko, O.; Shelby, T.; Banerjee, T.; Santra, S. A Comparison of Optical, Electrochemical, Magnetic, and Colorimetric Point-of-Care Biosensors for Infectious DiseaseDiagnosis. *ACS Infect. Dis.* **2018**, *4*, 1162−1178.
(22) Ghorbani, F.; Abbaszadeh, H.; Dolatabadi, J. E. N.; Aghebati-Maleki, L.; Yousefi, M. Application of Various Optical and Electrochemical Aptasensors for Detection of Human Prostate Specific Antigen: A Review. *Biosens. Bioelectron.* **2019**, *142*, 111484.
(23) Susan van, D.; Beulens, J. W. J.; Van der, S. Y. T.; Grobbee, D. E.; Nealb, B. The Global Burden of Diabetes and its Complications: An Emerging Pandemic. *Eur. J. Prev. Cardiol.* **2010**, *17*, No. s3.
(24) Khan, M. A. B.; Hashim, M. J.; King, J. K.; Govender, R. D.; Mustafa, H.; Al Kaabi, J. Epidemiology of Type 2 Diabetes − Global Burden of Disease and Forecasted Trends. *J. Epidemiol. Glob. Health* **2020**, *10*, 107−111.
(25) Saeedi, P.; Petersohn, I.; Salpea, P.; Malanda, B.; Karuranga, S.; Unwin, N.; Colagiuri, S.; Guariguata, L.; Motala, A. A.; Ogurtsova, K.; Shaw, J. E.; Bright, D.; Williams, R. ; Global and Regional Diabetes Prevalence Estimates for 2019 and Projections for 2030 and 2045: Results from the International Diabetes Federation Diabetes Atlas, 9thEdition. *Diabetes Res. Clin. Pract.* **2019**, *157*, 107843.
(26) Haffner, S. M. Diabetes, Hyperlipidaemia, and Coronary Artery Disease. *Am. J. Cardiol.* **1999**, *83*, 17−21.
(27) Moore, E. M.; Mander, A. G.; Ames, D.; Kotowicz, M. A.; Carne, R. P.; Brodaty, H.; Woodward, M.; Boundy, K.; Ellis, K. A.; Bush, A. I.; Faux, N. G.; Martins, R.; Szoeke, C.; Rowe, C.; Watters, D. A. Increased Risk of Cognitive Impairment in Patients with Diabetes is Associated with Metformin. *Diabetes Care* **2013**, *36*, 2981−2987.
(28) Neal, B.; Perkovic, V.; Mahaffey, K. W.; Zeeuw, D. D.; Fulcher, G.; Erondu, N.; Shaw, W.; Law, G.; Desai, M.; Matthews, D. R. Canagliflozin and Cardiovascular and Renal Events in Type 2 Diabetes. *N. Engl. J. Med.* **2017**, *377*, 644−657.
(29) Tuomilehto, J.; Lindstrom, J.; Eriksson, J. G.; Valle, T. T.; Hamalainen, H.; Ilanne-Parikka, P.; Keinanen-Kiukaanniemi, S.; Laakso, M.; Louheranta, A.; Rastas, M.; Salminen, V.; Uusitupa, M.; et al. Prevention of Type 2 Diabetes Mellitus by Changes in Lifestyle Among Subjects with Impaired Glucose Tolerance. *N. Engl. J. Med.* **2001**, *344*, 1343−1350.
(30) Hunt, J. A.; Gray, C. H.; Thorogood, D. E. Enzyme Tests for the Detection of Glucose. *Br. Med. J.* **1956**, *2*, 586−588.
(31) McMilin, J. M. Blood Glucose. In *Clinical Methods: The History, Physical and Laboratory Examinations*, 3rd ed.; Walker, H. K., Hall, W. D., Hurst, J. W., Eds.; Butterworth-Heinemann: Boston, MA, 1990.
(32) Kim, J.; Campbell, A. S.; Wang, J. Wearable Non-Invasive Epidermal Glucose Sensors: A Review. *Talanta* **2018**, *177*, 163−170.
(33) Gonzales, W. V.; Mobashsher, A. T.; Abbosh, A. The Progress of Glucose Monitoring - A Review of Invasive to Minimally and Non-Invasive Techniques, Devices and Sensors. *Sensors* **2019**, *19*, 800.
(34) Ballerstadt, R.; Schultz, J. S. A Fluorescence Affinity Hollow Fiber Sensor for Continuous Transdermal Glucose Monitoring. *Anal. Chem.* **2000**, *72*, 4185−4192.
(35) Caduff, A.; Hirt, E.; Feldman, Y.; Ali, Z.; Heinemann, L. First Human Experiments with a Novel Non-Invasive, Non-Optical Continuous Glucose Monitoring System. *Biosens. Bioelectron.* **2003**, *19*, 209−217.
(36) Rodbard, D. Continuous Glucose Monitoring: A Review of Successes, Challenges, and Opportunities. *Diabetes Technol. Ther.* **2016**, *18*, S2-3−S2-13.
(37) Kovatchev, B. P.; Cox, D. J.; Gonder-Frederick, L. A.; Clarke, W. L. Evaluating the Accuracy of Continuous Glucose-Monitoring Sensors. *Diabetes Care* **2004**, *27*, 1922−1928.
(38) Danne, T.; Nimri, R.; Battelino, T.; Bergenstal, R. M.; Close, K. L.; DeVries, J. H.; Garg, S.; Heinemann, L.; Hirsch, I.; Amiel, S. A.; Beck, R.; Bosi, E.; Buckingham, B.; Cobelli, C.; Dassau, E.; Doyle, F. J.; Heller, S.; Hovorka, R.; Jia, W.; Jones, T.; Kordonouri, O.; Kovatchev, B.; Kowalski, A.; Laffel, L.; Maahs, D.; Murphy, H. R.; Nørgaard, K.; Parkin, C. G.; Renard, E.; Saboo, B.; Scharf, M.; Tamborlane, W. V.; Weinzimer, S. A.; Phillip, M. International Consensus on Use of Continuous Glucose Monitoring. *Diabetes Care* **2017**, *40*, 1631−1640.

https://doi.org/10.1021/acsbiomaterials.1c00830
ACS Biomater. Sci. Eng. XXXX, XXX, XXX−XXX

(39) Fabra, E. M.; Diez, J. L.; Bondia, J.; Sanz, A. J. L. A Comprehensive Review of Continuous Glucose Monitoring Accuracy during Exercise Periods. *Sensors* **2021**, *21*, 479.
(40) Sierra, J. F.; Galban, J.; Castillo, J. R. Determination of Glucose in Blood Based on the Intrinsic Fluorescence of Glucose Oxidase. *Anal. Chem.* **1997**, *69*, 1471−1476.
(41) Rossi, L. M.; Quach, A. D.; Rosenzweig, Z. Glucose Oxidase−Magnetite Nanoparticle Bioconjugate for Glucose Sensing. *Anal. Bioanal. Chem.* **2004**, *380*, 606−613.
(42) Sanz, V.; de Marcos, S.; Galban, J. Direct Glucose Determination in Blood Using a Reagentless Optical Biosensor. *Biosens. Bioelectron.* **2007**, *22*, 2876−2883.
(43) Doong, R.; Shih, H. Array-Based Titanium Dioxide Biosensors for Ratiometric Determination of Glucose, Glutamate and Urea. *Biosens. Bioelectron.* **2010**, *25*, 1439−1446.
(44) Eggert, H.; Frederiksen, J.; Morin, C.; Norrild, J. C. J. A New Glucose-Selective Fluorescent Bisboronic Acid. First Report of Strong α-Furanose Complexation in Aqueous Solution at Physiological pH. *J. Org. Chem.* **1999**, *64*, 3846−3852.
(45) Murtaza, Z.; Tolosa, L.; Harms, P.; Lakowicz, J. R. On the Possibility of Glucose Sensing Using Boronic Acid and a Luminescent Ruthenium Metal−Ligand Complex. *J. Fluoresc.* **2002**, *12*, 187−192.
(46) Alexeev, V. L.; Sharma, A. C.; Goponenko, A. V.; Das, S.; Lednev, I. K.; Wilcox, C. S.; Finegold, D. N.; Asher, S. A. High Ionic Strength Glucose-Sensing Photonic Crystal. *Anal. Chem.* **2003**, *75*, 2316−2323.
(47) Suri, J. T.; Cordes, D. B.; Cappuccio, F. E.; Wessling, R. A.; Singaram, B. Continuous Glucose Sensing with a Fluorescent Thin Film Hydrogel. *Angew. Chem., Int. Ed.* **2003**, *42*, 5857−5859.
(48) Kanekiyo, Y.; Tao, H. Selective Glucose Sensing Utilizing Complexation with Fluorescent Boronic Acid on Polycation. *Chem. Lett.* **2005**, *34*, 196−197.
(49) Cordes, D. B.; Gamsey, S.; Singaram, B. Fluorescent Quantum Dots with Boronic Acid Substituted Viologens to Sense Glucose in Aqueous Solution. *Angew. Chem., Int. Ed.* **2006**, *45*, 3829−3832.
(50) Schiller, A.; Wessling, R. A.; Singaram, B. A Fluorescent Sensor Array for Saccharides Based on Boronic Acid Appended Bipyridinium salts. *Angew. Chem., Int. Ed.* **2007**, *46*, 6457−6459.
(51) Yu, C.; Yam, V. W. W. Glucose Sensing Via Polyanion Formation and Induced Pyrene ExcimerEmission. *Chem. Commun.* **2009**, 1347−1349.
(52) Tierney, S.; Falch, B. M. H.; Hjelme, D. R.; Stokke, B. T. Determination of Glucose Levels Using a Functionalized Hydrogel-Optical Fiber Biosensor: Toward Continuous Monitoring of Blood Glucose in Vivo. *Anal. Chem.* **2009**, *81*, 3630−3636.
(53) Shibata, H.; Heo, Y. J.; Okitsu, T.; Matsunaga, Y.; Kawanishi, T.; Takeuchi, S. Injectable Hydrogel Microbeads for Fluorescence-Based in Vivo Continuous Glucose Monitoring. *Proc. Natl. Acad. Sci. U. S. A.* **2010**, *107*, 17894−17898.
(54) Wu, W.; Mitra, N.; Yan, E. C. Y.; Zhou, S. Multifunctional Hybrid Nanogel for Integration of Optical Glucose Sensing and Self-Regulated Insulin Release at Physiological pH. *ACS Nano* **2010**, *4*, 4831−4839.
(55) Hargrove, A. E.; Ellington, A. D.; Anslyn, E. V.; Sessler, J. L. Chemical Functionalization of Oligodeoxynucleotides with Multiple Boronic Acids for the Polyvalent Binding of Saccharides. *Bioconjugate Chem.* **2011**, *22*, 388−396.
(56) Kumai, M.; Kozuka, S.; Samizo, M.; Hashimoto, T.; Suzuki, I.; Hayashita, T. Glucose Recognition by a Supramolecular Complex of Boronic Acid Fluorophore with Boronic Acid-Modified Cyclodextrin in Water. *Anal. Sci.* **2012**, *28*, 121.
(57) Huang, Y. J.; Ouyang, W. J.; Wu, X.; Li, Z.; Fossey, J. S.; James, T. D.; Jiang, Y. B. Glucose Sensing via Aggregation and the Use of "Knock-Out" Binding to Improve Selectivity. *J. Am. Chem. Soc.* **2013**, *135*, 1700−1703.
(58) Wu, X.; Li, Z.; Chen, X. X.; Fossey, J. S.; James, T. D.; Jiang, Y. B. Selective Sensing of Saccharides Using Simple BoronicAcids and Their Aggregates. *Chem. Soc. Rev.* **2013**, *42*, 8032−8048.
(59) Wu, X.; Chen, X. X.; Jiang, Y. B. Recent Advances in Boronic Acid-Based OpticalChemosensors. *Analyst* **2017**, *142*, 1403−1414.
(60) Mansouri, S.; Schultz, J. S. A Miniature Optical GlucoseSensor Based on Affinity Binding. *Nat. Biotechnol.* **1984**, *2*, 885−890.
(61) Ballerstadt, R.; Schultz, J. S. A Fluorescence Affinity HollowFiber Sensor for Continuous Transdermal Glucose Monitoring. *Anal. Chem.* **2000**, *72*, 4185−4192.
(62) Cummins, B. M.; Lim, J.; Simanek, E. E.; Pishko, M. V.; Cote, G. L. Encapsulation of a Concanavalin A/Dendrimer Glucose Sensing Assay within Microporated Poly(ethylene glycol)Microspheres. *Biomed. Opt. Express* **2011**, *2*, 1243−1257.
(63) D'Auria, S.; Herman, P.; Rossi, M.; Lakowicz, J. R. The Fluorescence Emission of the Apo-Glucose Oxidase from Aspergillus Niger as Probe to Estimate Glucose Concentrations. *Biochem. Biophys. Res. Commun.* **1999**, *263*, 550−553.
(64) Chinnayelka, S.; McShane, M. J. Microcapsule Biosensors Using Competitive Binding Resonance Energy Transfer Assays Based on Apoenzymes. *Anal. Chem.* **2005**, *77*, 5501−5511.
(65) Zhao, X.; Zou, X.; Ye, L. Controlled pH- and Glucose-Responsive Drug Release Behavior of Cationic Chitosan Based Nano-Composite Hydrogels by Using Graphene Oxide as Drug Nano-carrier. *J. Ind. Eng. Chem.* **2017**, *49*, 36−45.
(66) Teodorescu, F.; Oz, Y.; Queniat, G.; Abderrahmani, A.; Foulon, C.; Lecoeur, M.; Sanyal, R.; Sanyal, A.; Boukherroub, R.; Szunerits, S. Photothermally Triggered On-Demand Insulin Release from Reduced Graphene Oxide Modified Hydrogels. *J. Controlled Release* **2017**, *246*, 164−173.
(67) Cash, K. J.; Clark, H. A. Nanosensors and Nanomaterials for Monitoring Glucose in Diabetes. *Trends Mol. Med.* **2010**, *16*, 584−593.
(68) Zhang, Y.; Li, J.; Wu, M.; Guo, Z.; Tan, D.; Zhou, X.; Li, Y.; Liu, S.; Xue, L.; Lei, Y. Glucose-Responsive Gold Nanocluster-Loaded Microneedle Patch for Type 1 Diabetes Therapy. *ACS Appl. Bio Mater.* **2020**, *3*, 8640−8649.
(69) Zhao, Y.; Trewyn, B. G.; Slowing, I. I.; Lin, V. S. Y. Mesoporous Silica Nanoparticle-Based Double Drug Delivery System for Glucose-Responsive Controlled Release of Insulin and Cyclic AMP. *J. Am. Chem. Soc.* **2009**, *131*, 8398−8400.
(70) Sinha, A.; Chakraborty, A.; Jana, N. R. Dextran-Gated, Multifunctional Mesoporous Nanoparticle for Glucose Responsive and Targeted Drug Delivery. *ACS Appl. Mater. Interfaces* **2014**, *6*, 22183−22191.
(71) Hou, L.; Zheng, Y.; Wang, Y.; Hu, Y.; Shi, J.; Liu, Q.; Zhang, H.; Zhang, Z. Self-Regulated Carboxyphenylboronic Acid-Modified Mesoporous Silica Nanoparticles with "Touch Switch" Releasing Property for Insulin Delivery. *ACS Appl. Mater. Interfaces* **2018**, *10*, 21927−21938.
(72) Zhao, L.; Xiao, C.; Ding, J.; He, P.; Tang, Z.; Pang, X.; Zhuang, X.; Chen, X. Facile One-Pot Synthesis of Glucose-Sensitive Nanogel via Thiol-Ene Click Chemistry for Self-Regulated Drug Delivery. *Acta Biomater.* **2013**, *9*, 6535−6543.
(73) Zhao, L.; Xiao, C.; Ding, J.; Zhuang, X.; Gai, G.; Wang, L.; Chen, X. Competitive Binding-Accelerated Insulin Release from a Polypeptide Nanogel for Potential Therapy of Diabetes. *Polym. Chem.* **2015**, *6*, 3807−3815.
(74) Lee, D. Y.; Choe, K.; Jeong, Y. J.; Yoo, J.; Lee, S. M.; Park, J. H.; Kim, P.; Kim, Y. C. Establishment of a Controlled Insulin Delivery System Using a Glucose-Responsive Double-Layered Nanogel. *RSC Adv.* **2015**, *5*, 14482−14491.
(75) Dong, Y.; Wang, W.; Veiseh, O.; Appel, E. A.; Xue, K.; Webber, M. J.; Tang, B. C.; Yang, X. W.; Weir, G. C.; Langer, R.; Anderson, D. G. Injectable and Glucose-Responsive Hydrogels Based on Boronic Acid−Glucose Complexation. *Langmuir* **2016**, *32*, 8743−8747.
(76) Kim, M. Y.; Kim, J. Chitosan Microgels Embedded with Catalase Nanozyme-Loaded Mesocellular Silica Foam for Glucose-Responsive Drug Delivery. *ACS Biomater. Sci. Eng.* **2017**, *3*, 572−578.
(77) Wang, Y.; Zhang, X.; Han, Y.; Cheng, C.; Li, C. pH- and Glucose-Sensitive Glycopolymer Nanoparticles Based on Phenyl-

https://doi.org/10.1021/acsbiomaterials.1c00830
ACS Biomater. Sci. Eng. XXXX, XXX, XXX−XXX

boronic Acid for Triggered Release of Insulin. *Carbohydr. Polym.* **2012**, *89*, 124−131.
(78) Zhao, L.; Xiao, C.; Wang, L.; Gai, G.; Ding, J. Glucose-Sensitive Polymer Nanoparticles for Self-Regulated Drug Delivery. *Chem. Commun.* **2016**, *52*, 7633−7652.
(79) Jamwal, S.; Ram, B.; Ranote, S.; Dharela, R.; Chauhan, G. S. New Glucose Oxidase-Immobilized Stimuli-Responsive Dextran Nanoparticles for Insulin Delivery. *Int. J. Biol. Macromol.* **2019**, *123*, 968−978.
(80) Volpatti, L. R.; Matranga, M. A.; Cortinas, A. B.; Delcassian, D.; Daniel, K. B.; Langer, R.; Anderson, D. G. Glucose-Responsive Nanoparticles for Rapid and Extended Self-Regulated Insulin Delivery. *ACS Nano* **2020**, *14*, 488−497.
(81) Wang, B.; Ma, R.; Liu, G.; Li, Y.; Liu, X.; An, Y.; Shi, L. Glucose-Responsive Micelles from Self-Assembly of Poly(ethylene glycol)-b-Poly(acrylic acid-co-acrylamidophenylboronic acid) and the Controlled Release of Insulin. *Langmuir* **2009**, *25*, 12522−12528.
(82) Zhao, L.; Ding, J.; Xiao, C.; He, P.; Tang, Z.; Pang, X.; Zhuang, X.; Chen, X. Glucose-Sensitive Polypeptide Micelles for Self-Regulated Insulin Release at Physiological pH. *J. Mater. Chem.* **2012**, *22*, 12319−12328.
(83) Liu, G.; Ma, R.; Ren, J.; Li, Z.; Zhang, H.; Zhang, Z.; An, Y.; Shi, L. A Glucose-Responsive Complex Polymeric Micelle Enabling Repeated On−Off Release and Insulin Protection. *Soft Matter* **2013**, *9*, 1636−1644.
(84) Yang, H.; Sun, X.; Liu, G.; Ma, R.; Li, Z.; An, Y.; Shi, L. Glucose-Responsive Complex Micelles for Self-Regulated Release of Insulin Under Physiological Conditions. *Soft Matter* **2013**, *9*, 8589−8599.
(85) Li, L.; Jiang, G.; Du, X.; Chen, H.; Liu, Y.; Huang, Q.; Kong, X.; Yao, J. Preparation of Glucose-Responsive and Fluorescent Micelles via a Combination of RAFT Polymerization and Chemoenzymatic Transesterification for Controlled Release of Insulin. *RSC Adv.* **2015**, *5*, 75766−75772.
(86) Gaballa, H.; Theato, P. Glucose-Responsive Polymeric Micelles via Boronic Acid−Diol Complexation for Insulin Delivery at Neutral pH. *Biomacromolecules* **2019**, *20*, 871−881.
(87) Jeong, B.; Bae, Y. H.; Kim, S. W. Drug Release from Biodegradable Injectable Thermosensitive Hydrogel of PEG−PLGA−PEG Triblock Copolymers. *J. Controlled Release* **2000**, *63*, 155−163.
(88) Kumari, A.; Yadav, S. K.; Yadav, S. C. Biodegradable Polymeric Nanoparticles Based Drug Delivery Systems. *Colloids Surf., B* **2010**, *75*, 1−18.
(89) Makadia, H. K.; Siegel, S. J. Poly Lactic-co-Glycolic Acid (PLGA) as Biodegradable Controlled Drug Delivery Carrier. *Polymers* **2011**, *3*, 1377−1397.
(90) Danhier, F.; Ansorena, E.; Silva, J. M.; Coco, R.; Le Breton, A.; Preat, V. PLGA-Based Nanoparticles: An Overview of Biomedical Applications. *J. Controlled Release* **2012**, *161*, 505−522.
(91) Cho, H.; Gao, J.; Kwon, G. S. PEG-*b*-PLA Micelles and PLGA-*b*-PEG-*b*-PLGA Sol-Gels for Drug Delivery. *J. Controlled Release* **2016**, *240*, 191−201.
(92) Saha, A.; Basiruddin, S. K.; Maity, A. R.; Jana, N. R. Synthesis of Nanobioconjugates with a Controlled Average Number of Biomolecules between 1 and 100 per Nanoparticle and Observation of Multivalency Dependent Interaction with Proteins and Cells. *Langmuir* **2013**, *29*, 13917−13924.
(93) Dalal, C.; Saha, A.; Jana, N. R. Nanoparticle Multivalency Directed Shifting of Cellular Uptake Mechanism. *J. Phys. Chem. C* **2016**, *120*, 6778−6786.
(94) Saha, A.; Mohanta, S. C.; Deka, K.; Deb, P.; Devi, P. S. Surface-Engineered Multifunctional Eu: Gd_2O_3 Nanoplates for Targeted and pH-Responsive Drug Delivery and Imaging Applications. *ACS Appl. Mater. Interfaces* **2017**, *9*, 4126−4141.
(95) Santander-Ortega, M. J.; Jodar-Reyes, A. B.; Csaba, N.; Bastos-Gonzalez, D.; Ortega-Vinuesa, J. L. Colloidal Stability of Pluronic F68-Coated PLGA Nanoparticles: A Variety of Stabilisation Mechanisms. *J. Colloid Interface Sci.* **2006**, *302*, 522−529.
(96) Li, Y. P.; Pei, Y. Y.; Zhang, X. Y.; Gu, Z. H.; Zhou, Z. H.; Yuan, W. F.; Zhou, J. J.; Zhu, J. H.; Gao, X. J. PEGylated PLGA Nanoparticles as Protein Carriers: Synthesis, Preparation and Biodistribution in Rats. *J. Controlled Release* **2001**, *71*, 203−211.
(97) Astete, C. E.; Sabliov, C. M. Synthesis and Characterization of PLGA Nanoparticles. *J. Biomater. Sci., Polym. Ed.* **2006**, *17*, 247−289.
(98) Hernandez-Giottonini, K. Y.; Rodriguez-Cordova, R. J.; Gutierrez-Valenzuela, C. A.; Penunuri-Miranda, O.; Zavala-Rivera, P.; Guerrero-German, P.; Lucero-Acuna, A. PLGA Nanoparticle Preparations by Emulsification and Nanoprecipitation Techniques: Effects of Formulation Parameters. *RSC Adv.* **2020**, *10*, 4218−4231.
(99) Smith, M. K.; Northrop, B. H. Vibrational Properties of Boroxine Anhydride and Boronate Ester Materials: Model Systems for the Diagnostic Characterization of Covalent Organic Frameworks. *Chem. Mater.* **2014**, *26*, 3781−3795.

https://doi.org/10.1021/acsbiomaterials.1c00830
ACS Biomater. Sci. Eng. XXXX, XXX, XXX−XXX